Paper N° 2568

Registration Code: S-U1459803926

SELECTION AND SCALING OF EARTHQUAKE RECORDS FOR NONLINEAR ANALYSIS OF MARGINAL WHARVES

JC. Pantoja(1), JC. Reyes(2), JP. Smith-Pardo(3)

(1) *Research assistant, Dept. of Civil and Environmental Engineering, Universidad de los Andes, Bogota, Colombia, ,jc.pantoja10@uniandes*

(2) *Associate Professor, Dept. of Civil and Environmental Engineering, Universidad de los Andes, Bogota, Colombia, jureyes@uniandes.edu.co.*

(3) *Associate Professor, Dept. of Civil and Environmental Engineering, Seattle University, Seattle, USA, smithjh@seattleu.edu*

Abstract

A recently developed scaling procedure called the modal pushover-based scaling (MPS) has been successfully implemented in the seismic analysis of single and multi-story buildings with symmetric or unsymmetrical structural plan distribution. In this investigation, MPS is implemented for three-dimensional computer models of four marginal wharves. The selected case-study structures, representative of current design practice for wharves in container terminals, are 315 m and 630 m long. Medium and soft soil conditions are evaluated for each case. The structures are subjected to sets of seven near-field records selected and scaled according to the MPS procedure. Nonlinear response history analyses are conducted and results compared against the benchmark values. The latter are defined as the median values of the engineering demand parameters (EDP) due to 30 near-field unscaled records. The ASCE/SEI 7-10 scaling procedure is also examined for comparison purposes. It is found that the MPS procedure provides better estimates of the expected EDPs. In all cases the ASCE7-10 scaling procedure produces subestimations of expected EDPs, with errors in maximum drift and material strain demands of up to 40% and 60% respectively. Because the performance acceptance in the new standard ASCE 61-14 (seismic design of piers and wharves) is solely based on strain limits, the ASCE7-10 scaling procedure could lead to unconservative results.

Keywords: modal pushover-based scaling; marginal wharves; performance-based design

1. Introduction

The recently released standard ASCE 61-14 [1] favors the use performance-based procedures for evaluating the seismic response new or existing marginal wharves. This may involve the execution of response history analyses (RHAs) for an ensemble of earthquake records to determine engineering demand parameters (EDPs) for validation of targeted performance criteria. Because earthquake records selected for RHAs often need to be scaled to a seismic hazard level under consideration, multiple approaches have been suggested over the years for that purpose. Kalkan and Chopra [2] for example developed the modal pushover-based scaling (MPS) procedure for selecting and scaling earthquake ground motion records in a form that is convenient for evaluating existing and new structures. This procedure explicitly considers structural strength, obtained from the first-"mode" pushover curve, and allows determining a scaling factor for each record to match a target value of the deformation of the first-"mode" inelastic SDF system. The MPS procedure has been proven to be accurate and efficient for low-, medium- and high-rise buildings with symmetric plan [3, 4, 5] subjected to one component of ground motion. Reyes and Chopra [6, 7, 8] extended the MPS procedure to two horizontal components of ground motion.

Recently, Reyes and Quintero [9] proposed a new version of the MPS procedure for single-story asymmetric-plan buildings. Reyes et al. [10] further extended this to multi-story asymmetric-plan buildings. In this paper the developed procedure is applied to marginal wharf structures and compared against the ASCE/SEI 7-10 [11] (ASCE7 hence-forth) ground motion scaling procedure. Based on results from four case studies involving two soil types, it is shown that the MPS procedure provides superior results than the ASCE/SEI 7-10 ground motion scaling procedure.

2. Modal-pushover scaling (MPS) procedure

The MPS procedure is implemented in three phases: (1) computation of target roof displacement and pushover analyses, (2) scaling phase, and (3) selection phase. A step-by-step list of the general procedure [9] is presented next.

2.1 Target roof displacement and pushover analyses

(1) For a given site, define the target spectra $\hat{A}_x$ and $\hat{A}_y$, in this study taken as the median of the 5-percent damped pseudo-acceleration response spectra of two components of the ground motions.
(2) Compute the natural frequencies ω_n (periods T_n) and modes ϕ_n of the first few modes of linear-elastic vibration of the structure. For each ground motion component direction (x or y), identify the first, second and third modes as the three modes with the largest effective modal mass. In the case of a one story structure –as a marginal wharf- it is possible that only one or two modes have the largest effective modal mass; in such case, only these few modes should be used.
(3) Develop the base shear-roof displacement, $V_{bn} - u_{rn}$, relationship or pushover curve by nonlinear static analysis of the structure subjected to the n^{th}-"mode" invariant force distribution given by Eq. (1):

$$s_n^* = \begin{bmatrix} \mathbf{m}\phi_{xn} \\ \mathbf{m}\phi_{yn} \\ \mathbf{I}_\mathrm{o}\phi_{\theta n} \end{bmatrix} \tag{1}$$

where $\mathbf{m}$ is a diagonal matrix of order N with $m_{jj} = m_j$, the mass lumped at the j^{th} floor level; $\mathbf{I}_O$ is a diagonal matrix of order N with $I_{ojj} = I_{oj}$, the moment of inertia of the jth floor diaphragm about a vertical axis through the center of mass (C.M.); and subvectors ϕ_{xn}, ϕ_{yn}, and $\phi_{\theta n}$ of the n^{th} mode ϕ_n represent x, y and θ components of ground motion, respectively. This step should be implemented only for the first three "modes" in the direction under consideration; this step could be omitted for the higher-"modes" if they are treated as linear-elastic [12, chapter 20].

(4) Idealize the $V_{bn} - u_{rn}$ pushover curve as a bilinear or trilinear curve, as appropriate, and convert it into the force-deformation, $(F_{sn}/L_n) - D_n$, relationship for the n^{th}-"mode" inelastic SDF system using the well-known formulations [12, chapter 20] shown in Eq. (2):

$$\frac{F_{sn}}{L_n} = \frac{V_{bn}}{M_n^*} \; ; D_n = \frac{u_{rn}}{\Gamma_n \phi_{rn}}; \Gamma = \frac{L_n}{M_n} = \frac{\phi_n^T \mathbf{M}\iota}{\phi_n^T \mathbf{M} \phi_n}; \quad \mathbf{M} = \begin{bmatrix} \mathbf{m} & 0 & 0 \\ 0 & \mathbf{m} & 0 \\ 0 & 0 & \mathbf{I}_o \end{bmatrix}; \; \iota_x = \begin{bmatrix} 1 \\ 0 \\ 0 \end{bmatrix}; \text{and } \iota_y = \begin{bmatrix} 0 \\ 1 \\ 0 \end{bmatrix}; \tag{2}$$

where F_{sn} is a nonlinear hysteretic function of the nth modal coordinate [12, chapter 20]; M_n^* is the effective modal mass for the n^{th}-"mode"; **1** and **0** are vectors of dimension *N* with all elements respectively equal to one and zero; and ϕ_{rn} is the value of ϕ_n at the roof.

(5) Establish the target roof displacement $\hat{u}_r$. For a system with known T_n, damping ratio ξ_n, and force-deformation curve (Step 3), determine the peak deformation D_n for the n^{th}-"mode" inelastic SDF system due to each of the unscaled ground motions $\ddot{u}_g(t)$ by solving: $\ddot{D}_n(t) + 2\xi_n\omega_n\dot{D}_n(t) + \frac{F_{sn}}{L_n} = -\ddot{u}_g(t) \rightarrow D_n$

Determine $\widehat{D}_n$ as the median of the D_n values. Calculate roof displacement in the direction under consideration of the n^{th}-"mode" as $\hat{u}_{rn} = \Gamma_n \phi_{rn} \widehat{D}_n$, and compute the roof displacement in the direction under consideration $\hat{u}_r$ from values of $\hat{u}_{rn}$ using a suitable modal combination method (e.g., complete quadratic combination). In practical applications, the target deformation $\widehat{D}_n$ can be computed as $\widehat{D}_n = C_{Rn}\widehat{D}_{no}$, where C_{Rn} is the inelastic deformation ratio, estimated from empirical equations [13], and $\widehat{D}_{no} = (T_n/2\pi)^2 \hat{A}_n$ with $\hat{A}_n$ is the target pseudo-spectral acceleration at period T_n.

2.2 Scaling phase

(6) Compute the scale factor *SF* for each record in the direction under consideration by solving the following nonlinear equation: $u_r - \hat{u}_r = 0$, where u_r is the peak roof displacement in the direction under consideration from the scaled records. Because this equation is nonlinear, *SF* cannot be determined *a priori*, but requires the following iterative procedure:

a) Select an initial value of the scale factor *SF*, and compute deformation $D_n(t)$ for the n^{th}-"mode" inelastic SDF due to the scaled record by solving: $\ddot{D}_n(t) + 2\xi_n\omega_n\dot{D}_n(t) + F_{sn}/L_n = -SF \times \ddot{u}_g(t) \quad \rightarrow D_n(t)$

b) Compute roof displacement of the n^{th}-"mode" in the direction under consideration: $u_{rn}(t) = \Gamma_n \phi_{rn} D_n(t)$

c) Compute roof displacement in the direction under consideration: $u_r = max(|\sum_n u_{rn}(t)|)$

d) Estimate error: $\varepsilon = u_r - \hat{u}_r$

e) Adjust the value of the scale factor *SF*, and repeat steps a) to d) until ε is less than a tolerance value.

In this study, step 6 was implemented by a numerical algorithm. By executing steps a) to e), separately for the x and y components of the record, scale factors SF_x and SF_y are determined. Note that pushover curves (step 4), and target roof displacement (step 5) will be different for the two horizontal components of the ground motion.

2.3 Selection phase

(7) Select the first *k* records with the lower values of

$Error = \frac{\hat{A} - SF_x A_x + \hat{A} - SF_y A_y}{max(\hat{A}_x - SF_x A_x + \hat{A}_x - SF_y A_y)} + \frac{\hat{A}_{T_n} - SF_x A_{x,T_n} + \hat{A}_{T_n} - SF_y A_{y,T_n}}{max(\hat{A}_{T_n} - SF_x A_{x,T_n} + \hat{A}_{T_n} - SF_y A_{y,T_n})}$, where $\hat{A}$, A_x and A_y are vectors of spectral values $\hat{A}_i$ at different periods T_i between $0.2T_1$ and $1.5T_1$; $\hat{A}_{T_n}$, A_{x,T_n} and A_{y,T_n} are vectors of spectral values for the first three periods of vibration $T_{n,i}$. For single story and multi-story building the criterion for ground motion selection is different as shown in [9, 10].

3. Ground motions

Table 1 lists the 30 ground motion records selected for this study. They corresponded to near-field earthquakes with moment magnitudes between 6.5 and 7.5, and fault distances ranging from 3.6 to 12.8 km. None of the records was pulse-like so near-fault effects were not expected to be have significant effect in the response of the structural models.

Table 1 – Ground motion records used in this study

ID	Earthquake Name	Year	Station Name	M_w	$R_{closest}$ [km]	NEHRP Site class
1	Imperial Valley-06	1979	El Centro Array No 8	6.5	3.9	D
2	Imperial Valley-06	1979	El Centro Differential Array	6.5	5.1	D
3	Imperial Valley-06	1979	EC County Center FF	6.5	7.3	D
4	Imperial Valley-06	1979	El Centro Array No 10	6.5	8.6	D
5	Superstition Hills-02	1987	Poe Road (temp)	6.5	11.2	D
6	Corinth Greece	1981	Corinth	6.6	10.3	C
7	Northridge-01	1994	Pacoima Kagel Canyon	6.7	7.3	C
8	Northridge-01	1994	Sun Valley - Roscoe Blvd	6.7	10.1	D
9	Northridge-01	1994	Canyon Country - W Lost Cany	6.7	12.4	D
10	Nahanni Canada	1985	Site 2	6.8	4.9	C
11	Nahanni Canada	1985	Site 1	6.8	9.6	C
12	Chuetsu-oki Japan	2007	Kawanishi Izumozaki	6.8	11.8	D
13	Gazli USSR	1976	Karakyr	6.8	5.5	D
14	Kobe Japan	1995	Nishi-Akashi	6.9	7.1	C
15	Loma Prieta	1989	Corralitos	6.9	3.9	C
16	Loma Prieta	1989	Saratoga - Aloha Ave	6.9	8.5	C
17	Loma Prieta	1989	Saratoga - W Valley Coll.	6.9	9.3	D
18	Loma Prieta	1989	Gilroy Array No 3	6.9	12.8	D
19	Imperial Valley-02	1940	El Centro Array No 9	7.0	6.1	D
20	Cape Mendocino	1992	Cape Mendocino	7.0	8.0	C
21	Cape Mendocino	1992	Bunker Hill FAA	7.0	12.2	C
22	Montenegro Yugoslavia	1979	Ulcinj - Hotel Albatros	7.1	4.4	C
23	Montenegro Yugoslavia	1979	Ulcinj - Hotel Olimpic	7.1	5.8	D
24	Montenegro Yugoslavia	1979	Bar-Skupstina Opstine	7.1	7.0	C
25	Hector Mine	1999	Hector	7.1	11.7	C
26	Duzce Turkey	1999	IRIGM 498	7.1	3.6	C
27	Duzce Turkey	1999	Duzce	7.1	6.6	D
28	Duzce Turkey	1999	Bolu	7.1	12.0	D
29	Landers	1992	Joshua Tree	7.3	11.0	C
30	Manjil Iran	1990	Abbar	7.4	12.6	C

All the records were first amplified by a factor of 1.5 to ensure that the models of the case study structures could be driven well into their nonlinear range of response under the simulated ground motions. These pre-amplified records (treated as "unscaled" in this investigation) were resolved into fault-parallel (FP) and fault-normal (FN) components and the corresponding pseudo-acceleration spectra were calculated as shown in Fig. 1 with light gray lines. For the purpose of evaluating the alternative selection and scaling procedures, the geometric mean spectrum of the 30 records -shown with a black line- was selected as the target pseudo-acceleration spectrum.

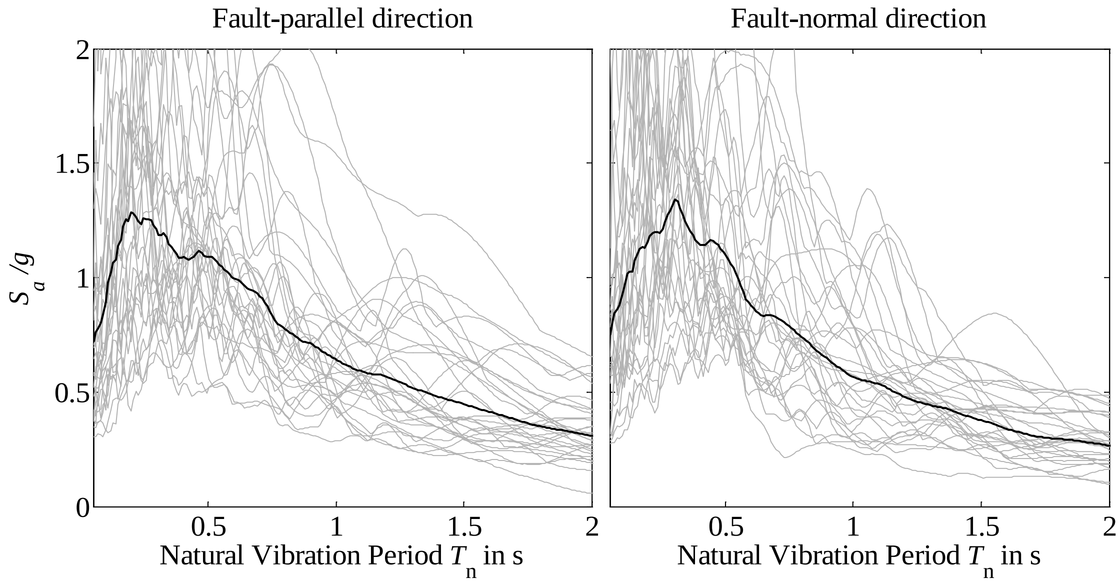

Fig. 1– Target spectra and response spectra for selected 30 ground motion records- 5% damping

4. Case study structures

Pile-supported waterfront facilities are long structures often conformed by transverse frames connected through a deck superstructure. In practice, these facilities are denominated as finger pier or marginal wharf depending on whether their longer plan dimension is perpendicular or parallel to the shoreline. Container wharves are commonly designed for large live loads of up 50 kN per square meter which combined with stringent durability requirements lead to the need for stiff and strong superstructures. Piles, on the other hand, are often long to reach competent load bearing soil layers while also accommodating the draft of modern container vessels. As a result, and contrary to the desired behavior of buildings, the condition of strong beam-weak column (pile) is inherent to this type of structure. Inelastic actions caused by ground motion excitation are particularly significant at the pile-to-cap interface of landside piles because these members are stiffer and connection capacity is usually smaller than that of the pile itself.

Cross-sectional views the case study structures are depicted in Figs. 2 and 3 and consists of marginal wharves supported on 610 mm (24 in.) square piles made of pre-stressed concrete. The first and second structure, henceforth denoted as Wharf 1 and Wharf 2, had 43 transverse bents at 7.5m on-centers. Wharf 3 and Wharf 4, on the other hand, consists of 85 transverse bents at 7.5m spacing. The two sets of facilities are representative of container terminals with the capability to respectively provide one and two berths for Panamax container vessels. Each structure has two longitudinal bents at 30.48 m (100 ft) on-center, which directly support the rails for ship-to-shore (STS) gantry cranes. Pile spacing in those longitudinal bents is 2.5 m only to support large crane wheel loads. The longitudinal (x) direction of each wharf was assumed to be parallel to the causative fault of the ground motion records while the FN component of each ground motion was assumed to be in the transverse (y) direction of the structure. The framing system consisted of piles and transverse pile caps that support 350mm- thick precast/prestressed concrete panels spanning in the longitudinal direction of the wharf. The panels and the pile caps have with sufficient transverse reinforcement projecting into a 200mm-thick cast-in-place (CIP) concrete topping to ensure composite behavior. Piles were pre-tensioned through 24-12.7mm (1/2 in.)-diameter grade 270 strands, while pile-to-cap connection consisted of 12-25mm (#8) longitudinal bars.

Soil conditions included in this study range from soft to medium dense clay as characterized by the properties listed in Table 2. For simplicity, a single layer of soil was considered in the analyses although the variation of physical properties with depth was also modeled. Mudline slopes were 1:2 and 1:3.5 (vertical to horizontal) in correspondence with the medium dense and soft soils conditions.

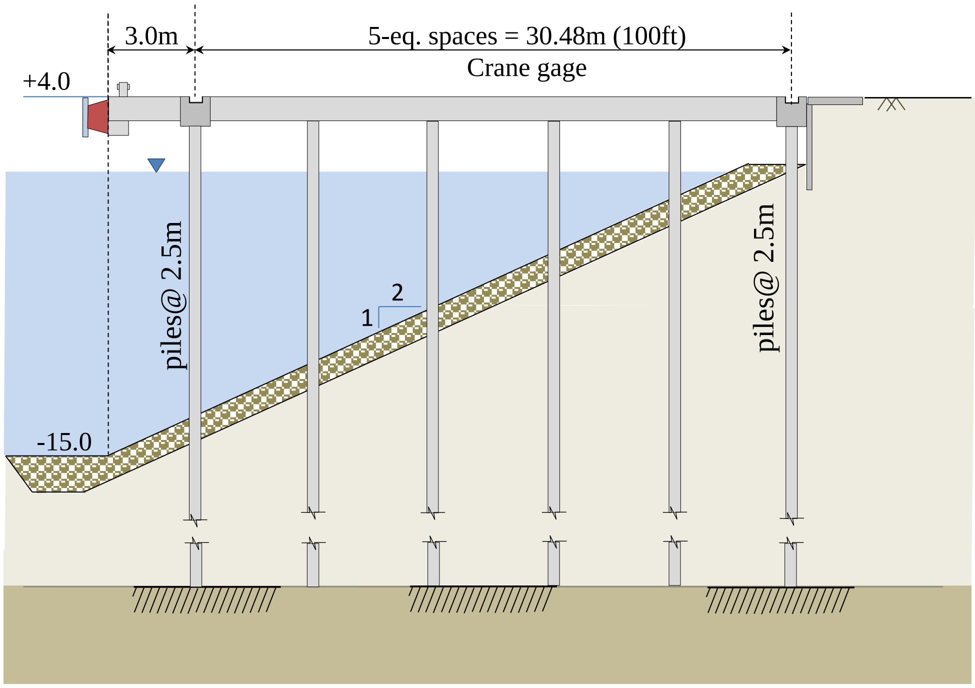

Fig. 2 – Cross-sectional view of case study structures on medium dense soil: Wharf 1 (315m long) and Wharf 3 (630m long)

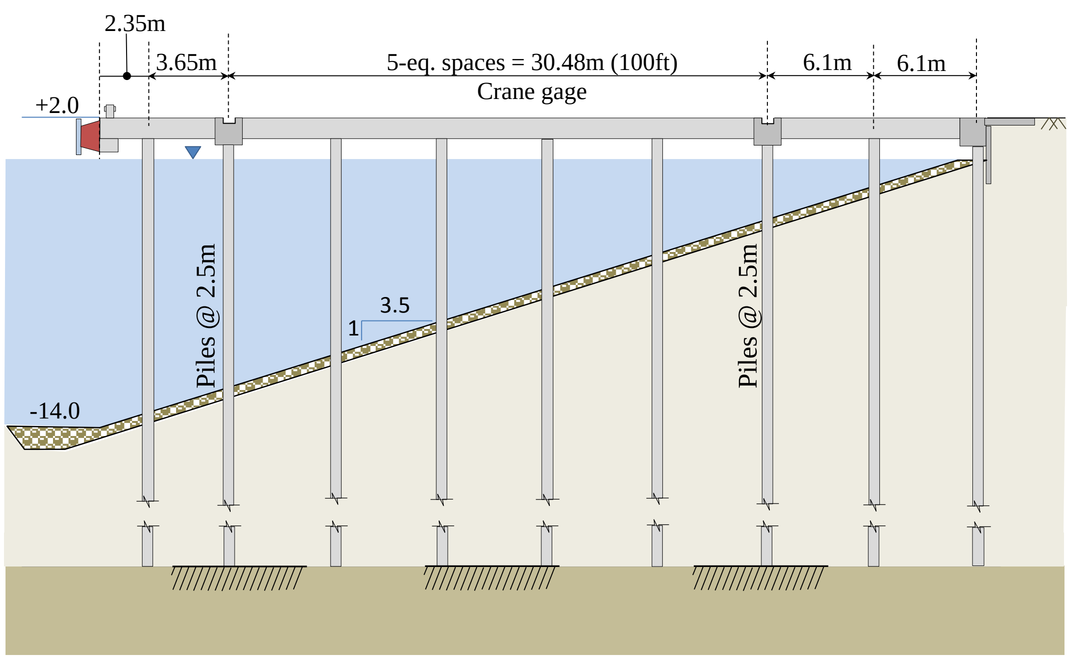

Fig. 3 – Cross-sectional view of case study structures on soft soil: Wharf 2 (315m long) and Wharf 4 (630m long)

Table 2 – Soil properties

Property	Soft soil (1:3.5 slope)	Medium dense soil (1:2 slope)
Unit weight, kN/m^3	20	20
Cohesion, kN/m^2	30	45
Friction angle, degree	18	22
Soil type	Soft clay	Clay

The case study structures were proportioned using ACI318-11 [14] for gravity loads and displacement-based provisions in standard ASCE 61-14[1] for seismic actions. Nonlinear response history analyses (RHA) of the case-study wharves were conducted using the program PERFORM 3D [15]. Three modeling alternatives were explored as described next.

- *Model alternative 1*: In this case nonlinear material fibers were used to represent piles and pile caps, while shell elements were used to model the deck panels. The restraining effect of the soil on the piles was represented using nonlinear lateral springs (also known as py-cuves) with force-displacement relations that depend on the depth [16, 17].
- *Model alternative 2*: In this case piles and pile caps were modeled as linear elastic elements with plastic hinges at their ends. Cycled strength deterioration and axial load-moment interaction were accounted for through the implementation of a model proposed by El-Tawil and Deierlein [18, 19]. Restraining effects of the supporting soil were again represented with py-curves.
- *Model alternative 3*: This is the least refined modeling alternative, which is also often used in consulting practice. Pile and pile caps were represented by linear elastic elements with plastic hinges at their ends. Soil nonlinear springs were not included in the analysis but instead piles were fixed at a certain depth below mudline. The depths to pile fixity were selected to produce similar force-displacement responses as compared to those from modeling alternatives 1 and 2.

Fig. 4 shows the pushover response of Wharf 1 in the transverse for the different modeling alternatives. The horizontal axis corresponds to the displacement at the center of mass while the vertical axis shows the base shear normalized by the weight of the structure. It can be observed that the comparison between the modeling options is favorable. Because the use of an equivalent fixed base for piles reduces the computational demand significantly, this alternative was used in the nonlinear RHAs.

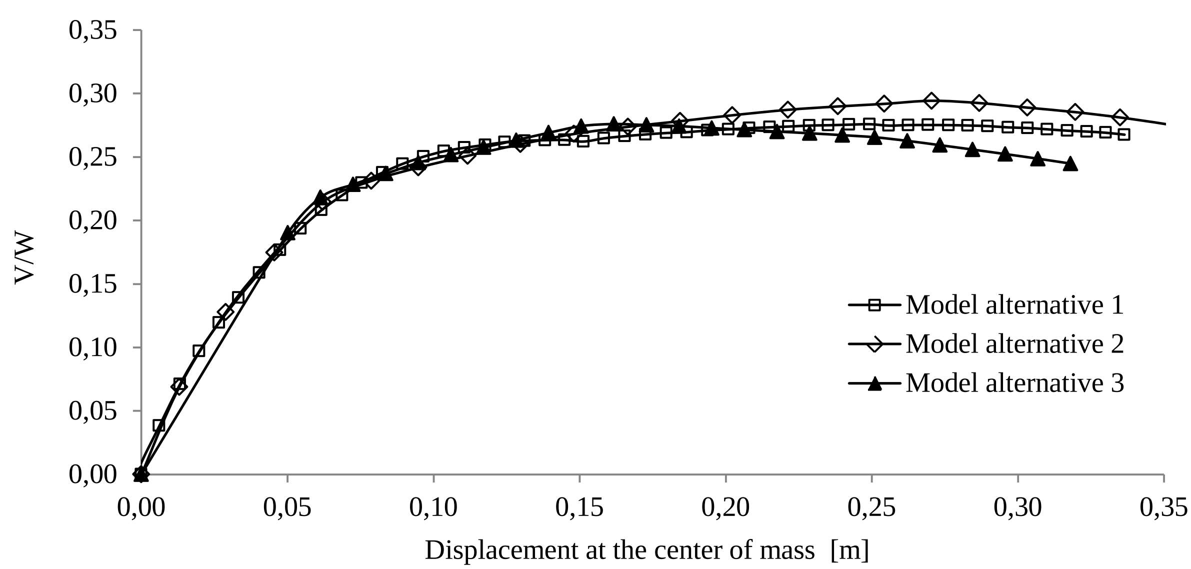

Fig. 4 – Pushover response of Wharf 1 In the transverse direction for different modeling alternatives

Figs. 5 and 6 shows the calculated effective modal mass along with a schematic representation of the first three mode shapes and corresponding periods of the four case-study structures with fixed bases (*Model Alternative 3*). It is observed that there is strong coupling between the longitudinal displacement and the plan rotation in the first and third mode, while transverse displacements dominate the second mode of vibration. These are consistent with the fact that the structure's center of stiffness is expected to be near the middle of the wharf in the longitudinal direction due to symmetry while in the transverse direction the center of stiffness is closer to the shorter (and stiffer) piles on the land side.

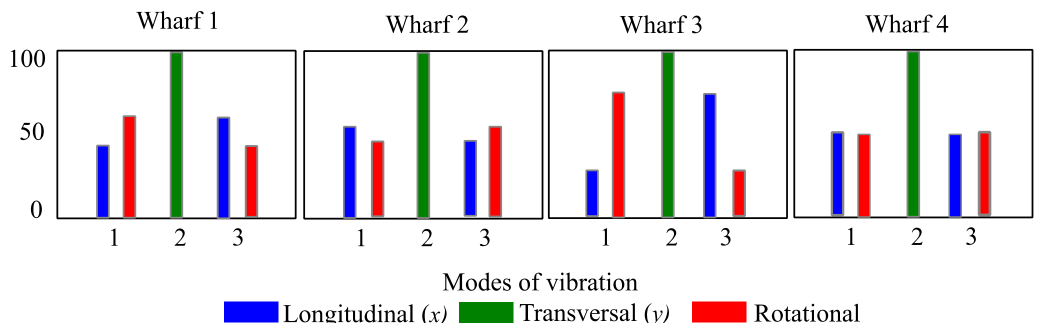

Fig. 5 – Effective modal mass for the case study structures

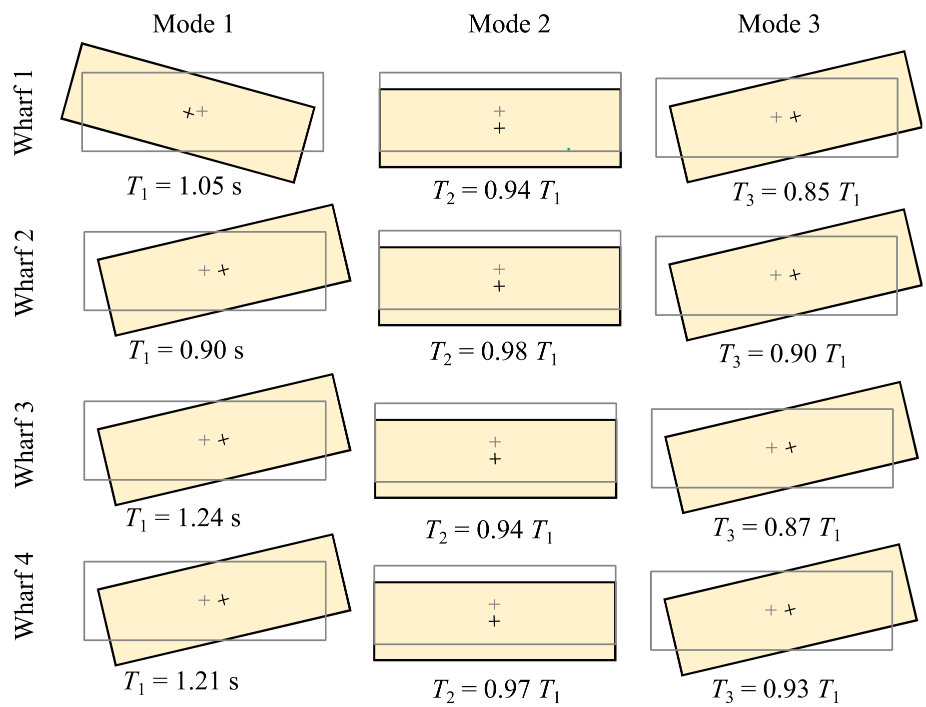

Fig. 6 – Schematics of the calculated first three mode shapes and periods of case study structures

5. Assessment of ASCE 7 and MPS procedures

The ASCE/SEI 7-10 and MPS procedures described in Section 2 were independently used to select and scale a set of seven ground motion records taken from those listed in Table 1. It was assumed that calculated EDPs of the case study structures are log-normally distributed. Evaluation of the procedures is reported in terms of accuracy and efficiency. Accuracy is measured by comparing the median of the calculated EDP for the case study structure subjected to seven scaled ground motion records with the calculated benchmark value. The latter is equal to median value of the EDP for the structure subjected to all 30 records listed in Table 1. Efficiency, on the other hand, is measured by the amount of dispersion in the calculated EDP.

Fig. 7 shows the calculated relative displacement, relative velocity and absolute acceleration at the center of mass for the case study structure as obtained from using the alternative scaling procedures and executing nonlinear time history analyses of the wharf models. In each case, the EDPs were normalized by the corresponding benchmark value, which is also listed in Table 3. The markers and vertical lines in this figure denote the median values of the EDPs plus or minus one standard deviation. It is observed that implementation of the ground motion scaling procedure prescribed in ASCE/SEI 7-10 produces underestimation of the benchmark displacements for the case study wharf structures by as much as 40%; thus, indicating that using the standard for this purpose may be unconservative. The MPS procedure, on the other hand, provides more accurate and conservative estimates of the benchmark values.

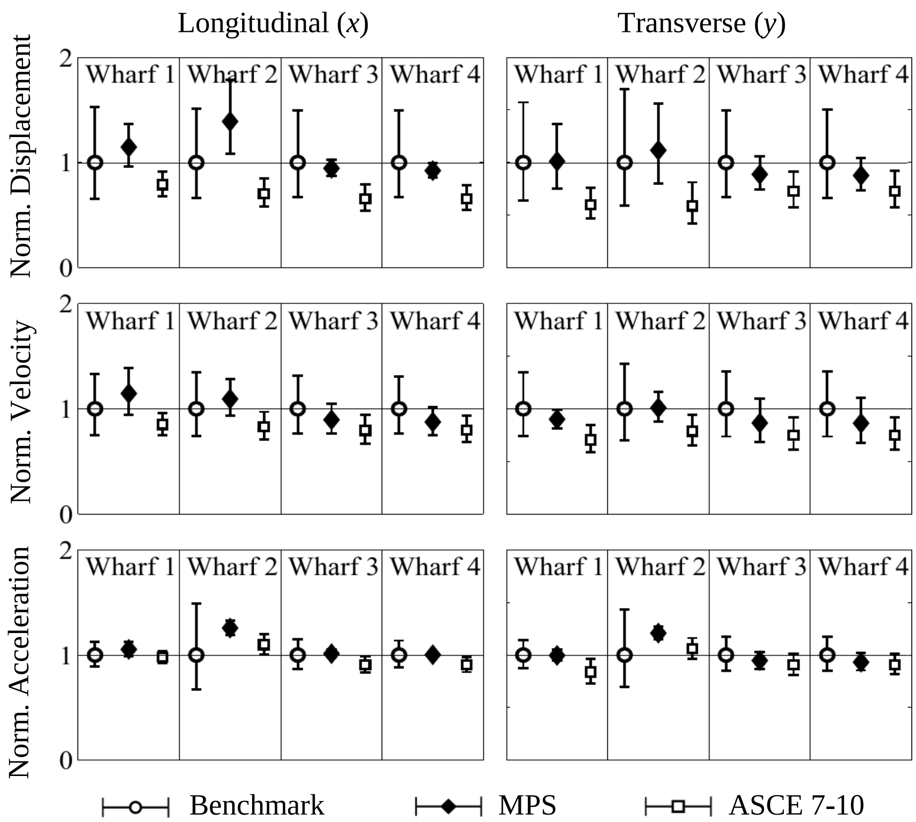

Fig. 7 – Normalized displacement, velocity and acceleration in the *x* and *y* direction at the C.M .of the case study wharves

Table 3 – Benchmark values at the C.M of the case structures

Wharf	Displacement m		Velocity m/s		Acceleration m/s^2	
	x	*y*	*x*	*y*	*x*	*y*
1	0.16	0.14	0.69	0.64	26.0	24.9
2	0.18	0.16	0.78	0.69	22.8	21.4
3	0.14	0.14	0.64	0.60	24.8	23.9
4	0.18	0.16	0.79	0.69	22.8	21.4

Fig. 8 shows the maximum calculated concrete and steel strain demands at the most critical pile-to-cap connections as obtained from nonlinear time history analyses of the case study structure models. Once again demands were normalized by the corresponding benchmark values, which are listed in Table 4. The locations of the reference points, schematically identified in the same table, correspond to the piles that are closest to the landside of the wharf and near the ends (P1 and P3) and middle (P2) in the longitudinal direction. The reasons for selecting these control points were mentioned in Section 4: landside piles are much stiffer than waterside piles due to shorter unsupported lengths; demands at the top of the piles are larger because of the stiff deck superstructure; and connections are usually weaker than the piles themselves.

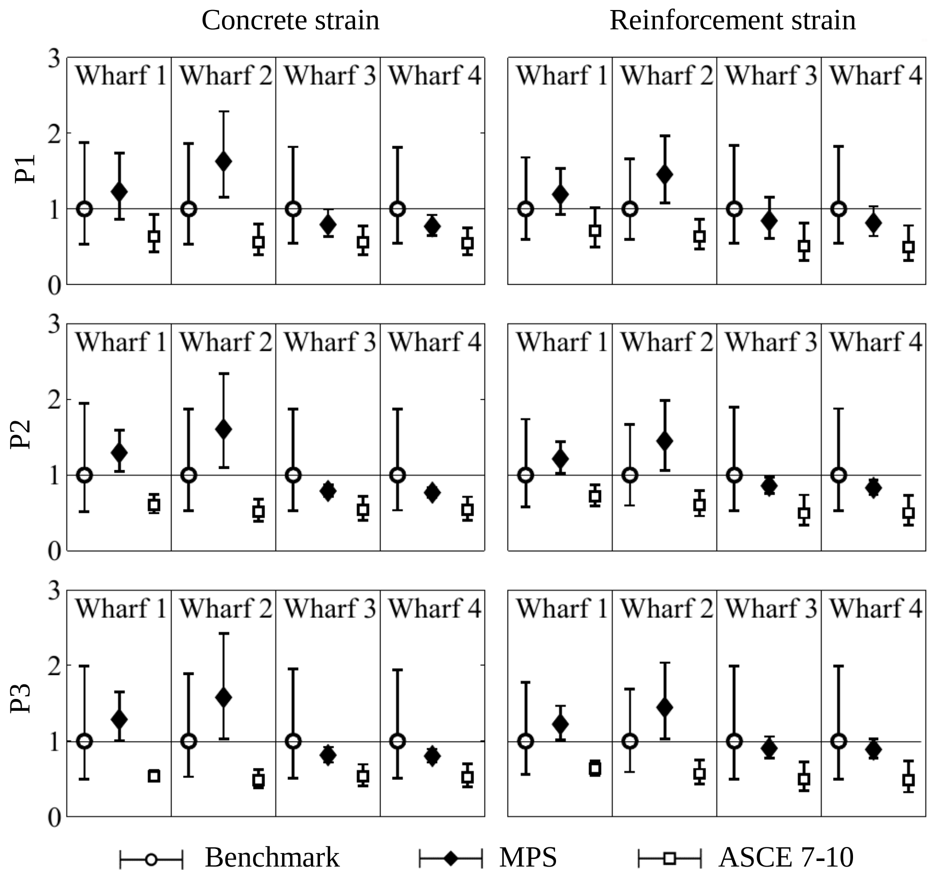

Fig. 8 – Maximum normalized concrete and reinforcement strain demands at various pile-to-cap connections

Table 4 – Calculated benchmark material strains (ε_c and ε_s for concrete and steel) at critical pile-to-cap connections [units = 1000μ]

Wharf	Connection					
	P_1		P_2		P_3	
	ε_c	ε_s	ε_c	ε_s	ε_c	ε_s
1	5.8	11.6	5.7	11.3	5.5	11.0
2	3.0	6.2	3.0	6.2	3.0	6.2
3	6.1	12.3	6.2	12.4	6.0	12.3
4	3.0	6.4	6.0	6.3	3.0	6.3

key

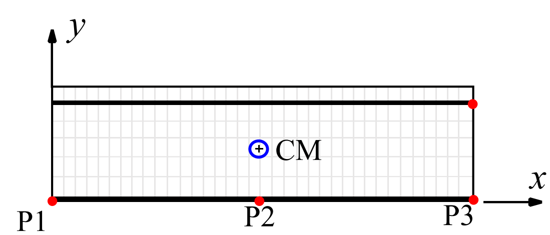

It is observed from Fig. 8 that material strain demands estimated using the ASCE/SEI7-10 ground motion scaling procedure are always smaller, by as much as 60%, than the corresponding benchmark values. Because these are the only performance criteria used in the standard for seismic design of piers and wharves (ASCE 61-14) the use of ground motions procedure in ASCE/SEI 7-10 proves to be unconservative for all the case study structures included in this investigation. By contrast, the MPS procedure provides reasonable and conservative estimates of benchmark values although with more dispersion. The authors believe that the reduced efficiency of the MPS procedure in this case may have to do with the mechanism of weak column (pile)/strong beam (pile cap) which is unconventional in relation to building structures. More research on the subject is required to develop modified versions of ground motion selection and scaling that could specifically apply to pile-supported wharves.

6. Summary and conclusions

ASCE/SEI 7-10 and MPS ground motion selection and scaling procedures were implemented in nonlinear response history analyses (RHA) of four 3D marginal wharf models that represent a wide range of practical applications. Calculated Engineering Demand Parameters (EPD) were compared against benchmark (median) values from RHA of the structure models under 30 ground motions defining a seismic scenario. It was found that implementing the ASCE/SEI 7-10 scaling procedure can result in underestimation of the platform drift demand by as much as 40% and underestimation of the material strain demands by as much as 60%. Because the latter is used as the performance indicator in the standard for the seismic design of pile-supported piers and wharves, it is concluded that scaling procedure included in ASCE/SEI 7-10 can provide significantly unconservative results. By contrast modal pushover-based scaling (MPS) was found to provide reasonably conservative estimates of benchmark values although with more dispersion.

7. References

[1] ASCE/COPRI 61-14 (2014): *Seismic design of piers and wharves*. American Society of Civil Engineers, Reston, Virginia.

[2] Kalkan E, Chopra AK. (2009) Modal Pushover-Based Ground Motion Scaling Procedure for Nonlinear Response History Analysis of Structures. Proceedings of the Structural Engineers Association of California Convention, San Diego, California.

[3] Kalkan E, Chopra AK. (2010) Practical guidelines to select and scale earthquake records for nonlinear response history analysis of structures, U.S. Geological Survey Open-File Report 2010-1068, available at http://pubs.usgs.gov/of/2010/1068/.

[4] Kalkan E, Chopra AK. (2011) Modal-pushover-based ground-motion scaling procedure. Journal of Structural Engineering 137(3):298-310.

[5] Kalkan E, Chopra AK. (2012) Evaluation of Modal Pushover-based Scaling of one Component of Ground Motion: Tall Buildings, Earthquake Spectra 28(4): 1469-1493.

[6] Reyes JC, Chopra AK. (2012)Modal Pushover-Based Scaling of Two Components of Ground Motion Records for Nonlinear RHA of Buildings. Earthquake Spectra 28(3):1243-1267.

[7] Reyes JC, Chopra AK. (2011) Three-dimensional modal pushover analysis of buildings subjected to two components of ground motion, including its evaluation for tall buildings. Earthquake Engineering and Structural Dynamics 40:789-806.

[8] Reyes JC, Chopra AK. (2011) Evaluation of three-dimensional modal pushover analysis for asymmetric-plan buildings subjected to two components of ground motion. Earthquake Engineering and Structural Dynamics 40:1475-1494.

[9] Reyes JC, Quintero O. (2014) Modal pushover-based scaling of earthquake records for nonlinear analysis of single-story asymmetric-plan buildings. Earthquake Engineering and Structural Dynamics 43:1005-1021.

[10] Reyes JC, Riaño AC, Kalkan E, Arango CM. (2014) Extending modal pushover-based scaling (MPS) procedure for nonlinear response history analysis of multi-story unsymmetric-plan buildings. Engineering Structures; (under revision).

[11] ASCE/SEI7-10 (2010): *Minimum design loads for buildings and other structures*. American Society of Civil Engineers, Reston Virginia.

[12] Chopra AK. (2007), Dynamics of Structures: Theory and Applications to Earthquake Engineering (4th edn.). Prentice-Hall:NJ.

[13] Chopra AK, Chintanapakdee C. (2004) Inelastic deformation ratios for design and evaluation of structures: Single-degree-of-freedom bilinear systems. ASCE J. Struct. Eng. 130(9): 1309–1319.

[14] ACI 318-11 (2011): Building code requirements for structural concrete. American Concrete Institute (ACI), Farmington hills, Michigan.

[15] PERFORM 3D (2006): *PERFORM 3D user guide v4*, Computers and Structures (CSI), Inc., Berkeley, California.

[16] Matlock H (1970): Correlations for design of laterally loaded piles in soft clay. *Offshore Technology Conference*, Houston.

[17] Reese LC, Cox WR, Koop F D (1974): Analysis of laterally loaded piles in sand. *Offshore Technology Conference*, Houston.

[18] El-Tawil S, Deierlein G (2001): Nonlinear analysis of mixed steel-concrete frames. I: element formulation. *Journal of Structural Engineering*, **127**(6), 647–55.

[19] El-Tawil S, Deierlein G (2001): Nonlinear analysis of mixed steel-concrete frames. II: implementation and verification. *Journal of Structural Engineering*, **127**(6), 656–65.